Void Ratio Effects on Lateral Stability of Rigid Poles Partially Embedded in Sands

ROBERT L. KONDNER, PAUL PFISTER and JOSEPH S. ZELASKO
Northwestern University

An investigation was made of the effects of void ratio on the lateral stability of rigid poles partially embedded in a saturated sand and subjected to a horizontal load applied a vertical distance, D, above the groundline. Void ratio effects are presented in terms of the dimensionless parameter, relative density. Nondimensional techniques in conjunction with small-scale model studies are used to determine the interrelationship among the physical variables. Tests were conducted in a quicksand tank device to control relative density. A response equation is given from which the load-deflection characteristics of a prototype pole might be estimated. The results have been compared with previous studies and satisfactory agreement was obtained. Explicit equations are given for certain circular poles, and expressions are developed for the ultimate value of the moment parameter and for the initial tangent modulus of the moment-deflection relation.

•NONDIMENSIONAL TECHNIQUES and small-scale model experiments are used to study the effect of relative density on the response of laterally loaded poles partially embedded in a cohesionless soil. A pole is considered a partially embedded rigid member whose deflections under load are primarily due to rigid body motions. Such poles are utilized in construction as anchorages, as well as by utilities, railroads, highway departments, etc. Failure of a pole is assumed to mean failure of the soil with excessive rotation of the pole since a proper structural design will avoid flexural failure of the pole itself. Because of the difficulty of associating the relative density to the elastic or elasto-plastic properties of a cohesionless soil, the problem is considered in terms of the physical variables involved using dimensional analysis. Although dimensional analysis in conjunction with small-scale model tests has not been extensively used in soil mechanics, there are instances of such studies (1, 2, 3). The present study is an extension of the work of Kondner et al. (2, 3).

THEORETICAL ANALYSIS

The general methods of dimensional analysis and the particular situations encountered in the field of soil mechanics when applying this tool have been previously described in detail by Kondner and Green (2) and are not discussed again here. The physical quantities considered are given in Table 1 in terms of a force-length-time system of fundamental units. Since there are twelve physical quantities and three fundamental units, there must be nine independent, nondimensional π terms. There is nothing unique about the form of the π terms and it is possible to transform them algebraically as long as the final π terms are nondimensional and independent.

The following nondimensional independent π terms were derived:

$$\pi_1' = \frac{X}{C}, \quad \pi_2' = \frac{M}{\gamma_d C^2 L^2}, \quad \pi_3' = \frac{C}{L}, \quad \pi_4' = \frac{D}{L}, \quad \pi_5' = \frac{C^2}{A},$$

$$\pi_6' = \phi, \quad \pi_7' = \frac{\gamma_d t C}{\eta}, \quad \pi_8' = D_r, \quad \pi_9' = \theta \qquad (1)$$

Paper sponsored by Committee on Mechanics of Earth Masses and Layered Systems.

TABLE 1

PHYSICAL QUANTITIES CONSIDERED IN DIMENSIONAL ANALYSIS OF RIGID POLE EMBEDDED IN SAND

Physical Quantity	Symbol	Fundamental Units
Horizontal deflection at groundline	X	L
Depth of embedment	L	L
Cross-sectional area of pole	A	L^2
Perimeter of pole	C	L
Moment arm (distance from groundline to point of load application)	D	L
Moment at groundline (product of load times moment arm)	M	FL
Dry density of sand	γ_d	FL^{-3}
Angle of internal friction	ϕ	$F^\circ L^\circ T^\circ$
Viscosity of sand	η	$FL^{-2}T$
Time of loading	t	T
Relative density	D_r	$F^\circ L^\circ T^\circ$
Rotation of pole	θ	$F^\circ L^\circ T^\circ$

Since the effect of variable density was the primary purpose of this study, and to avoid keeping too many terms in the final relationship, the π_2' termwas transformed into:

$$\pi_2 = \frac{M}{\gamma_d C^2 L^2} \times \frac{1}{1 + 2D_r} = \frac{M}{\gamma_d C^2 L^2 (1 + 2D_r)} \tag{2}$$

and π_8' became:

$$\pi_8'' = (1 + 2D_r) \tag{3}$$

and

$$\pi_8 = \frac{1 + 2D_r}{1 + 2D_r} = 1 \tag{4}$$

The term $(1 + 2D_r)$ was found, by experiment, to group the load-deflection curves for any series of tests in which only the density was varied into essentially one curve. This is shown by Figures 1 and 2. Figure 1 shows the dimensionless plots of $M/\gamma_d C^2 L^2$ vs X/C for three representative tests, the only difference being the relative density. Figure 2 indicates the applicability of the term $(1 + 2D_r)$ to collapse these curves. The variable γ_d is not a constant value for the three tests; however, its changes in magnitude are minor and are included in the final response formulation. Thus, the final set of π terms used for this study was:

$$\pi_1 = \frac{X}{C}, \quad \pi_2 = \frac{M}{\gamma_d C^2 L^2 (1 + 2D_r)}, \quad \pi_3 = \frac{C}{L}, \quad \pi_4 = \frac{D}{L},$$

$$\pi_5 = \frac{C^2}{A}, \quad \pi_6 = \phi, \quad \pi_7 = \frac{\gamma_d t C}{\eta}, \quad \pi_9 = \theta \tag{5}$$

The functional relationship developed using dimensional analysis has been written as:

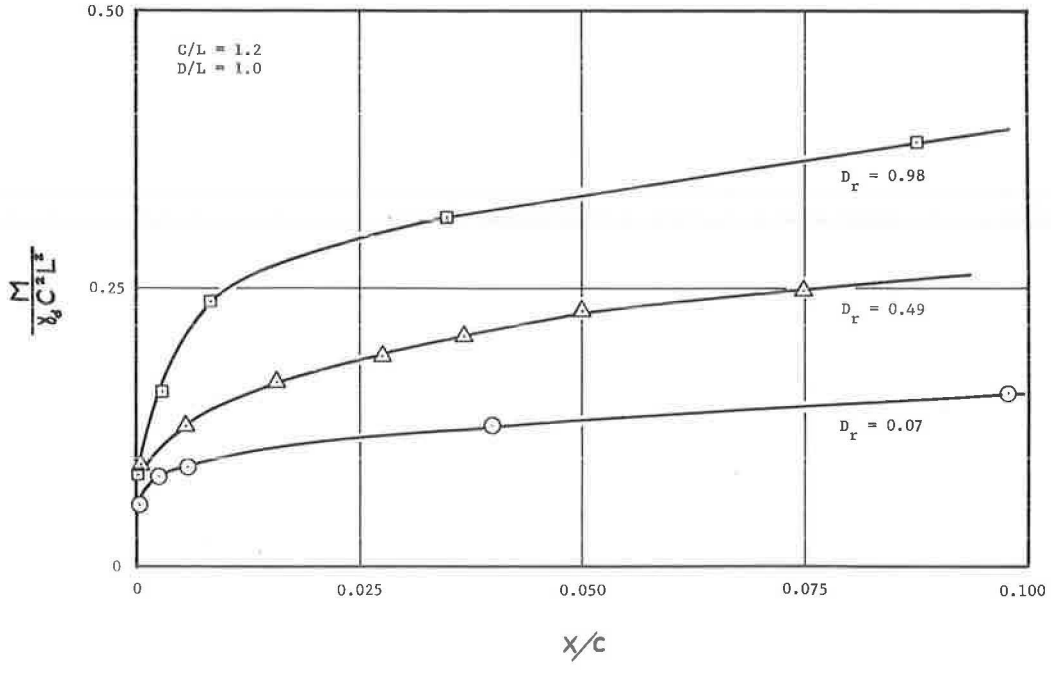

Figure 1. Preliminary form of moment-strength parameter vs X/C for various values of D_r.

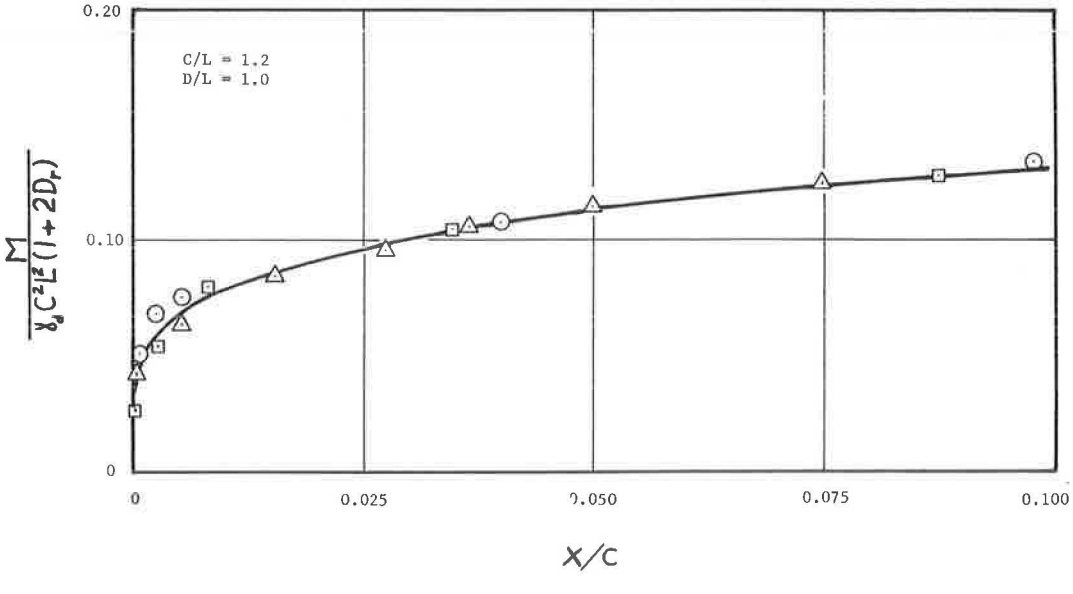

Figure 2. Final form of moment-strength parameter vs X/C for various values of D_r.

$$\frac{X}{C} = \varkappa \left[\frac{M}{\gamma_d C^2 L^2 (1 + 2D_r)}, \quad \frac{C}{L}, \quad \frac{D}{L}, \quad \frac{C^2}{A}, \quad \phi, \quad \frac{\gamma_d t C}{\eta}, \quad \theta \right] \tag{6}$$

The dependent variable is X/C, called a deflection ratio. Shape effects are included in the shape factor term C^2/A. By limiting the study to circular cross-sections, the value of C^2/A is a constant equal to 4π regardless of the size. The perimeter C is not necessarily the best choice of variable when dealing with irregular shapes, but this study is limited to circular poles. Additional work is needed to determine the most generally applicable form of this variable. The parameter D/L is a relative measure of moment arm to the embedment and is called the embedment ratio. The slenderness ratio is the term C/L. The parameter $M/\gamma_d C^2 L^2(1 + 2D_r)$, the moment-strength ratio, is the ratio of the applied moment to some form of strength parameter of the soil-pole system. The term $\gamma_d tC/\eta$ includes time effects; however, by proper choice of the loading rate, its effect can be minimized. For the present study, the rotation θ can be expressed in terms of the other geometric variables. A single sand was used in this study and variations in the angle of internal friction due to variations in void ratio were assumed to be accounted for in terms of the relative density. Thus, by restricting the problem to consideration of circular poles embedded in a particular sand and subjected to a proper load-time program, it is possible to simplify the functional relationship of Eq. 6 to the form:

$$\frac{X}{C} = \varkappa \left[\frac{M}{\gamma_d C^2 L^2 (1 + 2D_r)}, \quad \frac{C}{L}, \quad \frac{D}{L} \right] \tag{7}$$

EXPERIMENTAL PROCEDURE

Sand

The particular sand used was a medium to fine clean beach sand with a specific gravity of 2.70 and a gradation curve as shown in Figure 3. For its densest state, i.e., $D_r = 1.0$, its dry density was 108 pcf, and in its loosest state, i.e., $D_r = 0.0$, dry density was 96 pcf. Most experiments (an experiment being defined by a value of the embedment ratio D/L and a value of the slenderness ratio C/L) were run for relative densities of 1.0, 0.5 and 0.0, successively. Some tests were conducted for other values of D_r to check the validity of the moment-strength ratio parameter used for this study.

Model Poles

The model poles consisted of various lengths of polished aluminum or steel tube plugged at the lower ends. The properties of these poles are given in Table 2.

TABLE 2

PROPERTIES OF MODEL POLES

Pole No.	Material	Diameter		Area		Wt. (gm)	Perimeter	
		In.	Cm	Sq In.	Sq Cm		In.	Cm
1	Aluminum	0.501	1.273	0.197	1.263	30	1.573	3.996
2	Aluminum	0.626	1.590	0.307	1.981	62	1.966	4.993
3	Steel	0.707	1.796	0.393	2.535	143	2.221	5.641
4	Steel	0.927	2.355	0.674	4.349	216	2.911	7.394
5	Steel	1.248	3.170	1.222	7.819	229	3.921	9.959
6	Steel	1.515	3.848	1.801	11.619	478	4.755	12.077

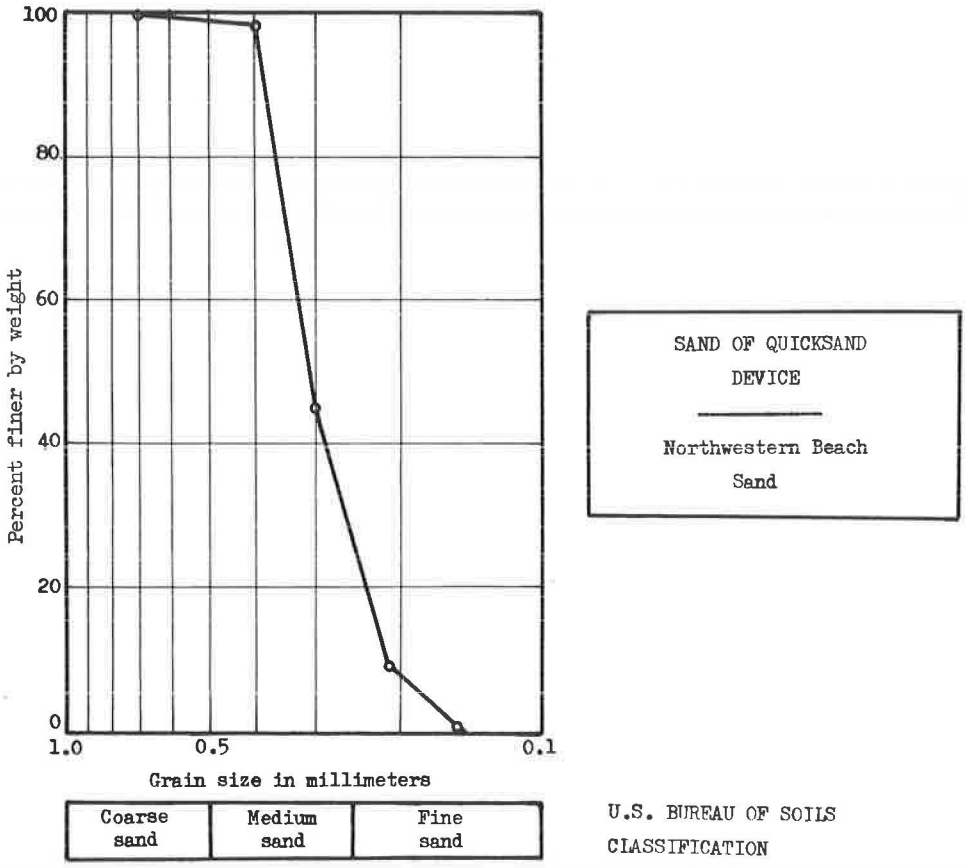

Figure 3. Grain size distribution of sand.

Apparatus

Because of the difficulty of obtaining a reasonable distribution of uniform intermediate values of void ratio (relative density) by compaction and vibratory methods, the so-called quicksand tank developed for quicksand and seepage experiments was used. This apparatus, a schematic diagram of which is shown in Figure 4, proved to be extremely convenient for the pole experiments. Water flowing upward at a controlled rate through the sand loosens it to its minimum density. To obtain any denser state of the sand, the tank walls were tapped with a rubber mallet so that the sand was densified by the applied shocks. Good reproducibility was obtained by this technique.

The tank contained 394 lb of oven-dried sand and the volume (hence, relative density) was determined from a previously obtained calibration curve by reading the height of the sand on scales placed at the four corners of the tank and averaging the readings. The load was applied to the model pole by hanging weights on a cord attached to the pole and passing over three small pulleys, as shown in Figure 4. Frictional forces in the apparatus were minimized and the internal springs in the indicator dials were removed. The sand was always in a saturated state with the level of the water slightly above the sand level.

TABLE 3

TESTS PERFORMED

C/L	D/L	D_r 1.0	D_r 0.5	D_r 0.0	Other
0.4	0.2	xx	x	x	
	0.4	xx	x	x	x
	0.6	xx	xx	xxx	
	0.8	xxx	xx	xx	
	1.0	xx	xxx	x	
	1.2	xx	xxx	x	
0.6	0.2	x		x	x
	0.4	x		x	
	0.6	x		x	x
	0.8	x		x	x
	1.0	x		x	x
	1.2	x		x	x
0.8	0.2	x	x	x	
	0.4	x	xx	x	
	0.6	x	x	x	
	0.8	xx	xx	x	x
	1.0	x	x	x	
	1.2	x	xx	x	
1.0	0.2	x	x	x	x
	0.4	xx	x	xx	
	0.6	x	x	x	
	0.8	x	x	x	
	1.0	x	x	xx	
	1.2	xx	x	xx	
1.2	0.2	x	x	x	xx
	0.4	x	x	x	
	0.6	x	x	x	x
	0.8	xx	xx	x	
	1.0	xx	x	x	
	1.2	xx	xx	xx	

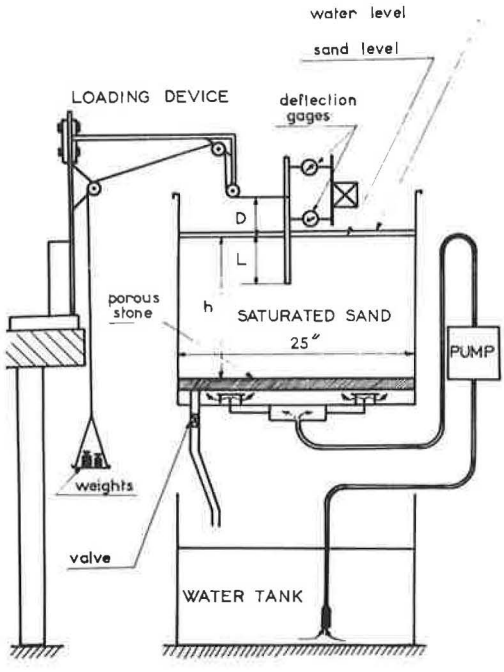

Figure 4. Schematic diagram of experimental apparatus.

EXPERIMENTAL RESULTS

The schedule of tests conducted is given in Table 3. Results of tests are shown in Figures 5 through 9 in terms of the parameters of Eq. 7; that is, the moment-strength ratio is plotted as a function of the deflection ratio X/C for various values of D/L for each particular value of C/L. Each curve represents an average of a number of tests. The experimental scatter about any single curve was quite small.

By using normalization functions for C/L and D/L, it was possible to normalize the response of Figures 5 through 9 to the particular response curve for C/L = 1.2 and D/L = 0.2, i.e., by first normalizing the various response curves for D/L to the D/L = 0.2 curve for each value of C/L by an appropriate function of D/L and then by collapsing the resulting curves which are only a function of C/L onto the C/L = 1.2 curve by another appropriate function. These normalization functions were determined to be a third-order and a second-order equation for D/L and C/L, respectively. Thus, the response can be written as:

$$\frac{M}{\gamma_d C^2 L^2 (1 + 2D_r)} = K_C K_D V_{(1.2 - 0.2)} \qquad (8)$$

where

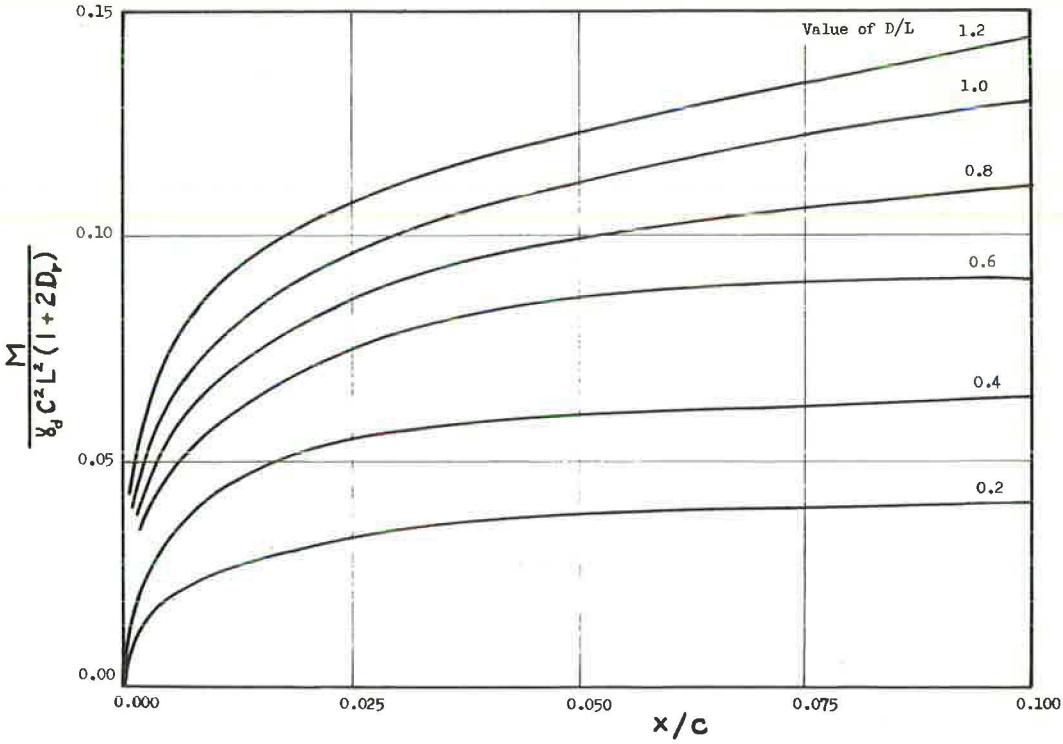

Figure 5. Moment-strength parameter vs X/C for various values of D/L; C/L = 1.2.

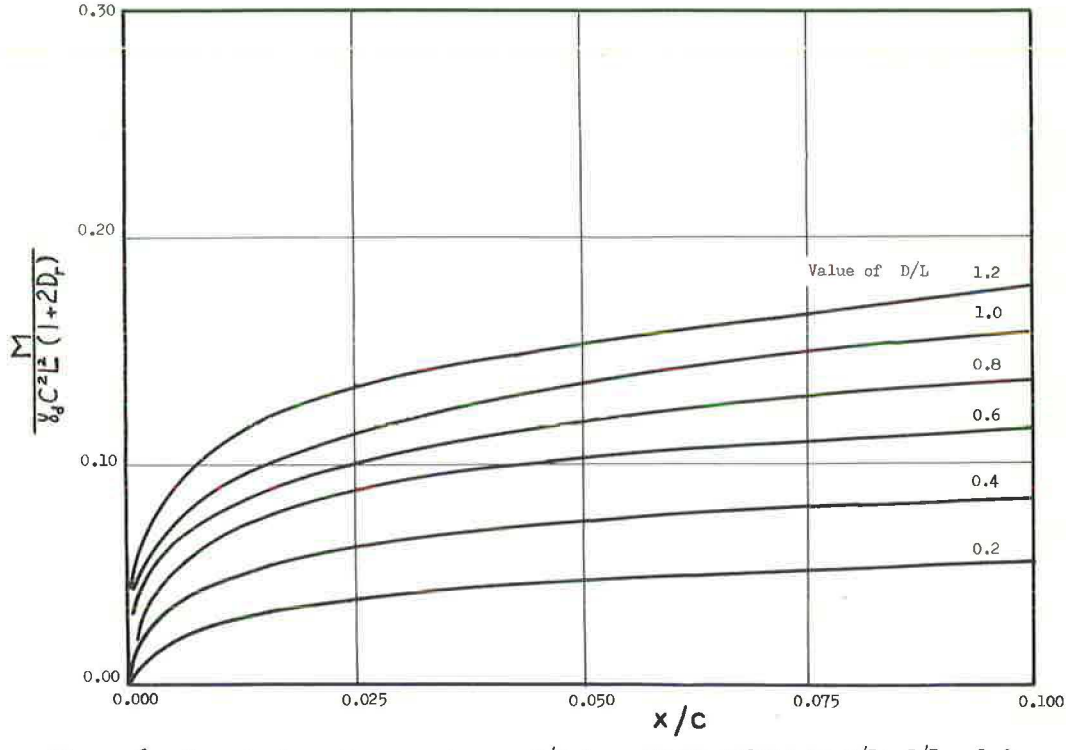

Figure 6. Moment-strength parameter vs X/C for various values of D/L; C/L = 1.0.

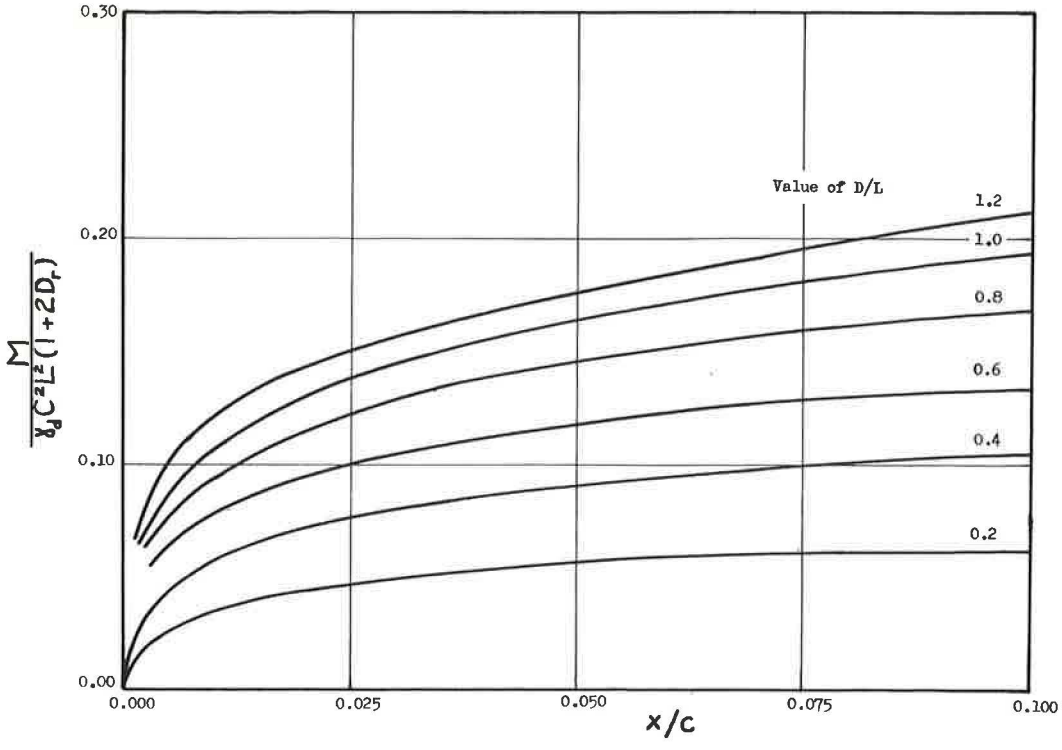

Figure 7. Moment-strength parameter vs X/C for various values of D/L; C/L = 0.8.

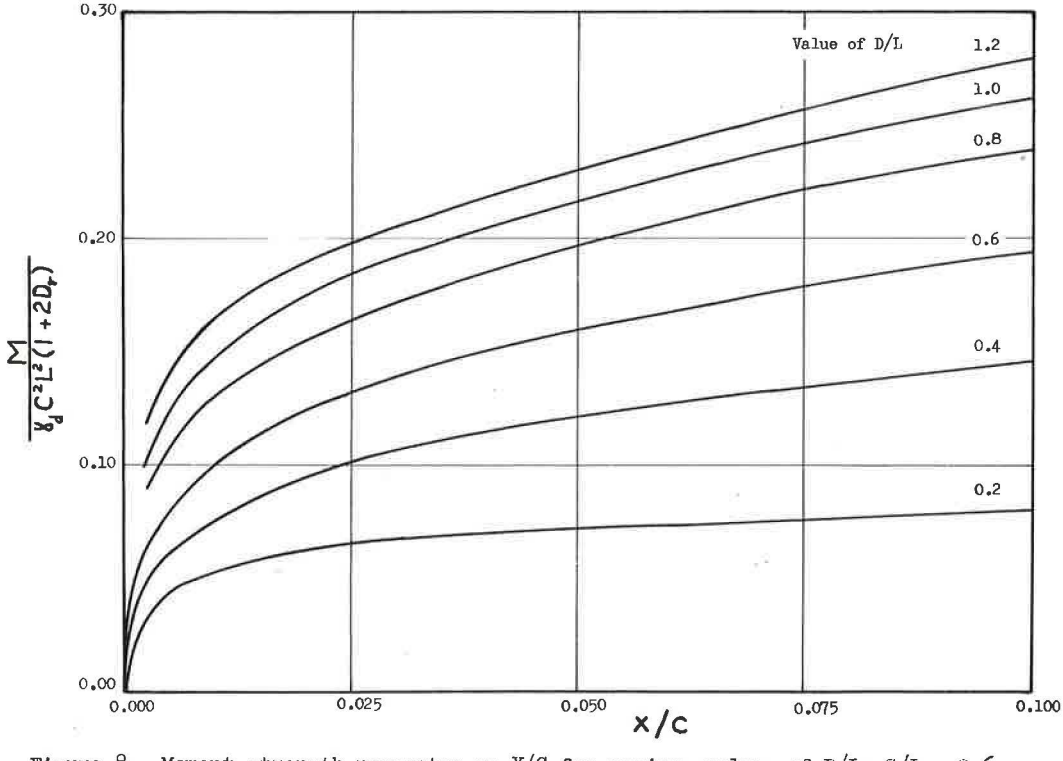

Figure 8. Moment-strength parameter vs X/C for various values of D/L; C/L = 0.6.

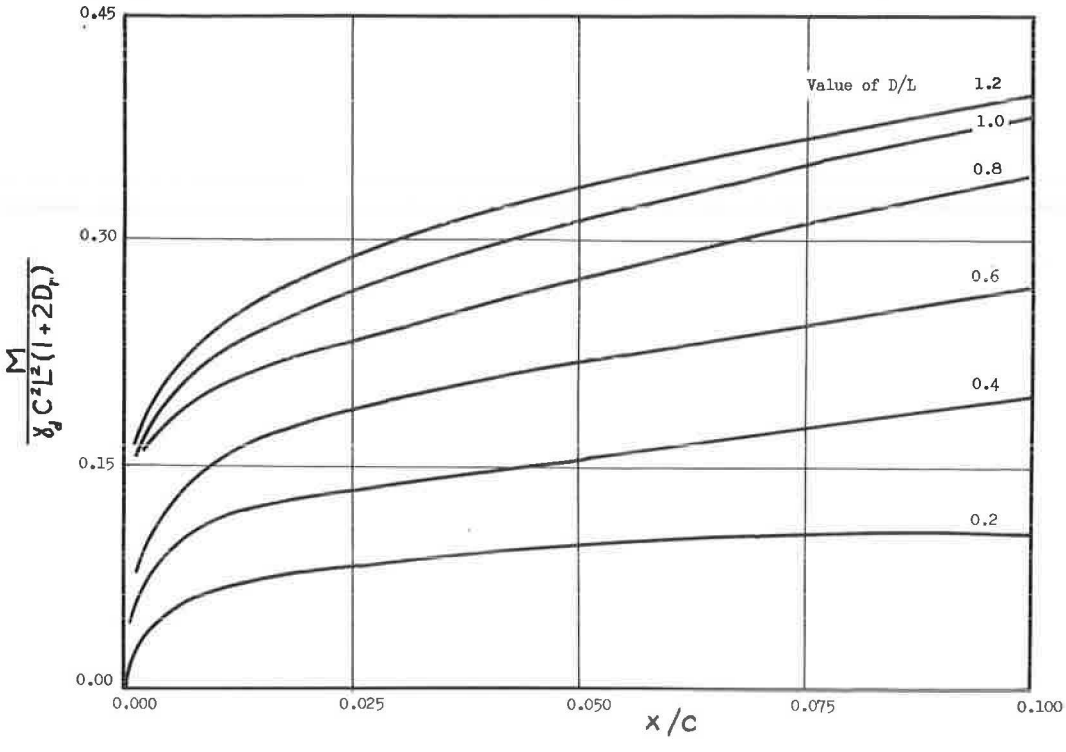

Figure 9. Moment-strength parameter vs X/C for various values of D/L; C/L = 0.4.

$$K_D = A\left(\frac{D}{L}\right)^3 + B\left(\frac{D}{L}\right)^2 + E\left(\frac{D}{L}\right) + F, \tag{9}$$

$$K_C = G\left(\frac{C}{L}\right)^2 + H\left(\frac{C}{L}\right) + J, \text{ and} \tag{10}$$

$V_{(1.2\ -\ 0.2)}$ = curve of moment-strength parameter vs X/C for C/L = 1.2 and D/L = 0.2.

For the particular sand tested, the numerical coefficients in Eqs. 9 and 10 are A = -0.563, B = 0.194, E = 3.087, F = 0.380, G = 2.476, H = -6.209, and J = 4.887.

If the curve of the moment-strength ratio vs the deflection ratio for C/L = 1.2 and D/L = 0.2 is plotted in terms of the transformed hyperbolic coordinates (4, 5), the response given in Figure 10 is obtained. This can be written as:

$$V_{(1.2\ -\ 0.2)} = \left[\frac{M}{\gamma_d C^2 L^2 (1 + 2D_r)}\right]_{\substack{C/L\ =\ 1.2 \\ D/L\ =\ 0.2}} = \frac{\frac{X}{C}}{a + b\frac{X}{C}} \tag{11}$$

where a = 0.175 and b = 22.532 are the slope and intercept, respectively, of the straight line of Figure 10. Physical interpretation can be attached to the constants a and b. Differentiation of Eq. 11 with respect to X/C and evaluation of the derivative at X/C = 0 gives:

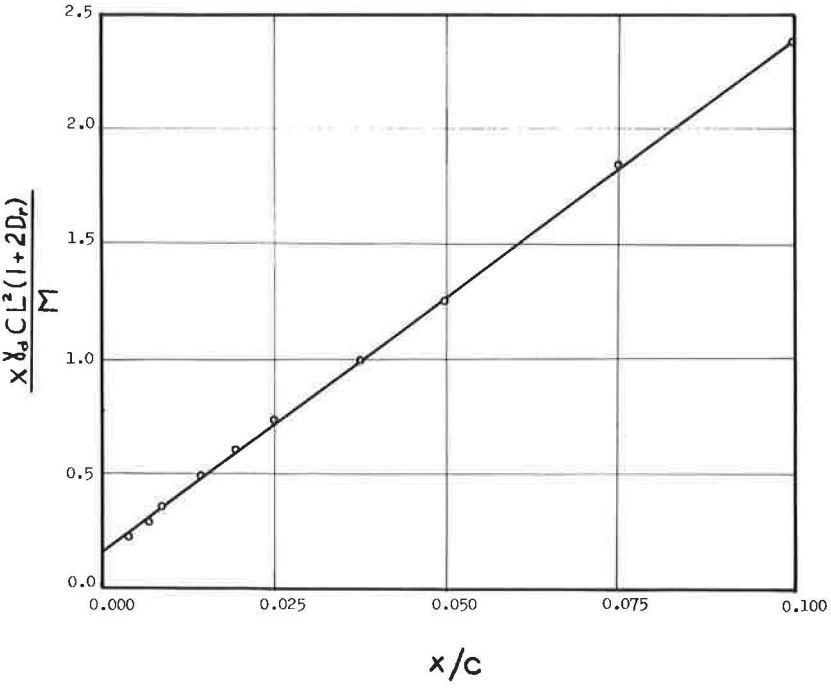

Figure 10. Transformed hyperbolic representation of moment-strength ratio vs X/C; C/L = 1.2; D/L = 0.2.

$$\left[\frac{dV_{(1.2\ -\ 0.2)}}{d\frac{X}{C}}\right]_{\frac{X}{C}\,=\,0} = \frac{1}{a} \tag{12}$$

Thus, the parameter 1/a represents a measure of the initial tangent modulus of the moment-strength ratio vs deflection ratio relation. The mathematical limit of Eq. 11 as the deflection parameter becomes excessive gives the theoretical ultimate value of the moment-strength ratio as 1/b:

$$\left[V_{(1.2\ -\ 0.2)}\right]_{ult} = \underset{\frac{X}{C}\to\infty}{\text{Lim}}\ V_{(1.2\ -\ 0.2)} = \frac{1}{b} \tag{13}$$

Thus, a measure of the initial tangent modulus of the deflection ratio vs moment-strength ratio obtained from Eq. 8 is $K_C K_D/a$, and the theoretical ultimate value of the moment-strength ratio can be written:

$$\left[\frac{M}{\gamma_d C^2 L^2 (1 + 2D_r)}\right]_{ult} = \frac{K_C K_D}{b} \tag{14}$$

The results obtained in this study and expressed in the form of Eqs. 8 through 11 agree well with the results reported by Shilts, Graves, and Driscoll (6) for both full-scale posts and large-scale model poles embedded in sand, and with the results reported

by Kondner and Cunningham (3) on small-scale model tests in dry sand. It is felt that the forms of these equations have some general applicability, but the particular values of the numerical coefficients given in this paper are limited to the present investigation. In addition, the reliability of these equations is felt to be better for the larger values of X/C.

The degree of saturation is an extremely important aspect to take into consideration when the magnitude of the numerical coefficients are obtained and utilized. Several experiments conducted by the authors in wet but not saturated sand showed that the force required for failure of a given pole at given values of C/L and D/L could be as much as 5 times larger under these conditions than under the condition of saturation used in this study. However, since a saturated situation is the most critical case and there is always the possibility of a partially saturated system becoming inundated, consideration of a sand-pole system should be conservative; hence, the saturated case is used.

SUMMARY OF METHOD

To use the method presented in this paper for a particular pole-soil system, the values of the numerical coefficients must be obtained from field tests.

Determination of a and b of Eq. 11

The parameters a and b are, respectively, the intercept and the slope obtained from a straight-line fit of a plot of $X_{\gamma d}CL^2(1 + 2D_r)/M$ vs X/C for a pole test with C/L = 1.2 and D/L = 0.2. Theoretically, only one test would be needed to determine the constants a and b; however, experimental error in conducting these tests indicates that a number of tests would be preferable to a single test.

Determination of A, B, E, and F

In addition to the test to obtain a and b (C/L = 1.2 and D/L = 0.2), three additional tests must be performed, e.g., C/L = 1.2 for D/L = 0.4, 0.8 and 1.2. Theoretically, these four tests will permit the calculation of the four constants A, B, E, and F. However, because of experimental error, a number of such tests would be desirable. By plotting the value of K_D of Eq. 9 as a function of D/L, intermediate values could be easily obtained.

Determination of G, H, and J

In addition to the test for C/L = 1.2 at D/L = 0.2, tests are needed for values of C/L = 0.4 and 0.8 at D/L = 0.2. These three tests can be used to determine the constants G, H, and J. Intermediate values could be obtained easily from a plot of K_C of Eq. 10 as a function of C/L.

It would be advisable to repeat each of these tests several times and to use the average curve.

CONCLUSIONS

1. The functional relationship given by Eq. 6 has been developed by the methods of dimensional analysis to describe the response of a rigid vertical pole partially embedded in sand and subjected to a horizontal load applied above the groundline. The various quantities of Eq. 6 are defined in Table 1.

2. Eqs. 8 through 11 represent the explicit form of the functional relationship as determined by small-scale model tests for circular poles embedded in a particular sand with $0.2 \leq D/L \leq 1.2$ and $0.4 \leq C/L \leq 1.2$. The form of these equations may be of considerable use in the study of prototype pole-soil systems. The values of the numerical coefficients in these equations are functions of the particular pole-soil systems and should be determined from field tests.

3. The theoretical ultimate value of the moment-strength ratio can be represented by Eq. 14 and the initial tangent modulus of the moment-strength ratio vs deflection parameter relation can be measured by $K_C K_D/a$.